Journal of Molecular Liquids 225 (2017) 856–862

Contents lists available at ScienceDirect

Journal of Molecular Liquids

journal homepage: www.elsevier.com/locate/molliq

MHD stagnation point Cattaneo–Christov heat flux in Williamson fluid flow with homogeneous–heterogeneous reactions and convective boundary condition — A numerical approach

M. Ramzan[a,*], M. Bilal[b], Jae Dong Chung[c]

[a]Department of Computer Science, Bahria University, Islamabad Campus, Islamabad44000, Pakistan
[b]Department of Mathematics, Faculty of Computing, Capital University of Science and Technology, Islamabad, Pakistan
[c]Department of Mechanical Engineering, Sejong University, Seoul143-747, Republic of Korea

ARTICLE INFO

Article history:
Received 17 September 2016
Accepted 31 October 2016
Available online 9 November 2016

Keywords:
Cattaneo–Christov heat flux model
Williamson fluid
Convective boundary condition
Magnetic field
Homogenous–heterogeneous reactions

ABSTRACT

In this study, we have explored numerical solution of two dimensional MHD stagnation point Williamson fluid flow under the influence of homogeneous–heterogeneous reactions over a linearly stretched surface. The flow is triggered by a linearly stretched surface with Cattaneo–Christov heat flux and convective boundary condition. Apposite transformations are betrothed to obtain ordinary differential equations with high nonlinearity. Shooting method is summoned to decipher system of differential equations. Graphs of different parameters against velocity, temperature and concentration profiles with relevant discussion are depicted emphasizing their physical significance. A comparison in limiting case is also featured in this investigation. It is found that effects of Williamson fluid parameter on velocity and temperature fields are conflicting.

1. Introduction

Non-Newtonian fluids are of great attention for researchers due to their enormous applications in industrial and engineering processes. Examples of non-Newtonian fluids may include pulps, sugar solutions, lubricants, apple sauce, tomato ketchup, shampoos, and lubricants. Unlike Newtonian fluids, in these fluids there is a nonlinear bond between deformation rate and shear stress. So, it is not possible to construct a relation explaining features of all non-Newtonian fluid models [1–10]. In non-Newtonian family tree, pseudo-plastic fluids are useful in many engineering applications like polymers and solutions with relatively higher molecular weight, coated photographic films, adhesives and emulsions . Cross model, Power law model, Carreaus model, Ellis model and Williamson model can be quoted as fluids with pseudo-plastic features. Amongst these, the Williamson fluid model has not yet been deliberated in detail. Williamson fluid model describes the flow of shear thinning non-Newtonian fluids. The industrial and biological liquids that obey the Williamson fluid are polymer melts/solutions, ketchup, blood, paint, whipped cream, nail polish, etc. Coined work of Williamson [11] who elucidated this model to express pseudo-plastic physiognomies with both characteristics of minimum and maximum viscosity motivated follower researchers to explore more fronts in this interesting non-Newtonian fluid category. Akbar et al. [12] found numerical solution of Williamson nanofluid flow using fourth and fifth order RK–Fehlberg method in an irregular channel. Nadeem et al. [13] examined Williamson fluid flow over a stretched surface using Homotopy Analysis method. Malik and Salahuddin [14] discussed numerical simulation of MHD Williamson fluid flow near stagnation point using RK–Fehlberg method over a stretched cylinder. Malik et al. [15] analyzed flow of Williamson fluid numerically with heat generation/absorption and variable thermal conductivity over a stretched cylinder using RK–Fehlberg method. Hayat et al. [16] highlighted Soret and Dufour impact in Williamson fluid flow under the influence of thermal radiation and viscous dissipation over an unsteady stretched surface. Hayat et al. [17] also studied Williamson fluid flow analytically using Homotopy Analysis method in attendance of viscous dissipation, Newtonian Joule and heating. Nadeem and Hussain [18] found series solution of Williamson nanofluid flow over a stretching sheet. Salahuddin et al. [19] explored numerical solution of MHD Williamson fluid flow with Cattaneo–Christov heat flux and variable thickness effects past a stretched surface. Prasannakumara et al. [20] established numerical solution of Williamson nanofluid flow past a stretched surface with

* Corresponding author.
E-mail address: mramzan@bahria.edu.pk (M. Ramzan).

http://dx.doi.org/10.1016/j.molliq.2016.10.139
0167-7322/

impact of chemical reaction in a porous medium. Effects of nonlinear thermal radiation are also taken into account.

Chemical reactions are categorized as homogeneous and heterogeneous. Homogeneous are where reactions and catalyst operate in the same phase but heterogeneous if they are in different phases. In general, processes involving homogeneous catalyst are in gaseous phase and in solid phase for heterogeneous catalyst. In case of production and consumption, it is reasonably difficult to predict relationship between homogeneous and heterogeneous reactions for reactant classes at varied rates with the same fluid and on surface of the catalyst. The importance of chemical reactions is more evident in different engineering applications like hydrometallurgical industry, food processing, manufacturing of ceramics, and groves of fruit trees and crops damage via freezing. Chaudhary and Merkin [21] examined stagnation point flow of viscous fluid with homogeneous and heterogeneous reactions. Later, they [22] improved their model by taking dissimilar diffusion coefficients for reactant and autocatalyst. Further, Merkin [23] discussed viscous fluid model with isothermal homogeneous and heterogeneous reactions. Khan and Pop [24] extended the work of Chaudhary and Merkin[21] by taking viscoelastic fluid. The model presented in Ref.[21] is deliberated with more insight by considering micropolar fluid passing through a permeable medium and a porous stretched surface by Shaw et al. [25]. Kameswaran et al. [26] studied vicious nanofluid flow with homogeneous and heterogeneous reactions past a permeable stretching surface. Some more recent attempts in this area are referred to Refs.[27–30].

Heat transfer mechanism is very useful because of its varied engineering applications like nuclear reactors for cooling purposes, magnetic drugs targeting, biomedical applications and cooling of energy production space. For the last two centuries, classical Fourier heat conduction law [31] was the only source to describe heat transfer process. However, a major constraint in Fourier's law named as Paradox of heat conduction was that the medium experienced an initial uproar immediately. This barrier was crossed by Cattaneo [32] who interleaved relaxation time to heat flux. Christov [33] improved Cattaneo's proposed model by swapping simple derivative with that of Oldroyd's upper convected derivative. Straughan [34] extended the work of Cattaneo–Christov by considering thermal convection in an incompressible viscous fluid with downward gravity. Ciarletta and Straughan [35] by considering Cattaneo–Christov equations, analyzed that in an unsteady problem, solution to the backward is highly depended on relaxation time. Mustafa [36] discussed flow of upper Maxwell fluid rotating flow with Cattaneo–Christov equations. Hayat et al. [37] presented a comparison of Cattaneo–Christov flux to that of Fourier heat conduction past viscoelastic fluid flow.

The present study examines Williamson fluid flow with effects of Cattaneo–Christov heat flux and convective boundary condition. In addition, homogeneous–heterogeneous reactions are also considered with magnetohydrodynamics near a stagnation point. Numerical solution is obtained for the problem using shooting technique. This problem is being undertaken for first time in literature as far as our knowledge is concerned. Graphical illustrations of varied prominent parameters versus velocity, temperature and concentration fields with requisite deliberation are also a part of this exploration. A comparison to previous study is also provided to validate obtained results.

2. Mathematical formulation

We presume flow of two dimensional MHD Williamson fluid with Cattaneo–Christov heat flux near stagnation point with convective boundary condition over a linearly stretched surface. The two temperatures on and away from the sheet are denoted by T_w and T_∞ with $T_w \geq T_\infty$. Magnetic field of strength B_o is applied upright to the stretched surface (see Fig. 1).

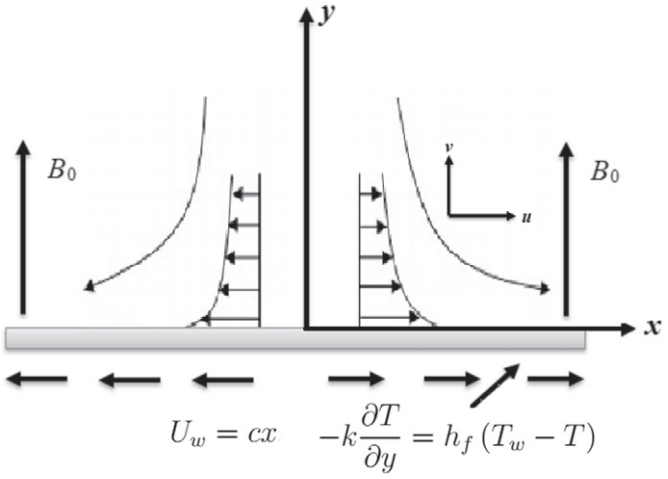

Fig. 1. Schematic flow diagram.

Polarization effects are ignored because peripheral electric field is absent. Eventually, assumption to consider small Reynold's number forced us to ignore induced magnetic field. Analysis is done in attendance of homogeneous–heterogeneous reactions. For cubic autocatalysis, homogeneous reaction is represented by

$$A + 2B \to 3B, \quad \text{rate} = k_c ab^2, \tag{1}$$

whereas on the surface of catalyst, the first order isothermal reaction is given by

$$A \to B, \quad \text{rate} = k_s a, \tag{2}$$

with k_c, k_s are the rate constants and a, b are concentrations of the different chemical classes, considering the fact that both reactions are of isothermal nature. As suggested in Ref.[19], boundary layer equations with respect to mass, momentum, energy and concentration are given by

$$\frac{\partial u}{\partial x} + \frac{\partial v}{\partial y} = 0, \tag{3}$$

$$u\frac{\partial u}{\partial x} + v\frac{\partial u}{\partial y} = u_e\frac{du_e}{dx} + \nu\frac{\partial^2 u}{\partial y^2} + \sqrt{2}\Gamma\nu\frac{\partial u}{\partial y}\frac{\partial^2 u}{\partial y^2} - \frac{\sigma B_o^2}{\rho}(u - u_e), \tag{4}$$

$$\rho C_P\left(u\frac{\partial T}{\partial x} + v\frac{\partial T}{\partial y}\right) = -\nabla.\mathbf{q}, \tag{5}$$

$$u\frac{\partial a}{\partial x} + v\frac{\partial a}{\partial y} = D_A\frac{\partial^2 a}{\partial y^2} - k_c ab^2, \tag{6}$$

$$u\frac{\partial b}{\partial x} + v\frac{\partial b}{\partial y} = D_B\frac{\partial^2 b}{\partial y^2} + k_c ab^2. \tag{7}$$

Here, u is along x-axis and v is along perpendicular axis. Moreover, $u_e, \Gamma, \nu, T, C_p, \rho, \mathbf{q}$ and D_A, D_B are variable external free stream velocity, time rate constant, kinematic viscosity, temperature, specific heat, fluid density, heat flux, heat flux, and diffusion coefficients of the species A and B respectively.

$$\mathbf{q} + \lambda_1\left(\frac{\partial \mathbf{q}}{\partial t} + \mathbf{V}.\nabla\mathbf{q} - \mathbf{q}.\nabla\mathbf{V} + (\nabla.\mathbf{V})\,\mathbf{q}\right) = -k\nabla T, \tag{8}$$

where k and λ_1 are fluid thermal conductivity and thermal relaxation time. Eliminating $\mathbf{q}$ from Eqs. (5) and (8) following Christov [33]

$$u\frac{\partial T}{\partial x}+v\frac{\partial T}{\partial y} = \frac{k}{\rho C_P}\frac{\partial^2 T}{\partial y^2}-\lambda_2\left(u^2\frac{\partial^2 T}{\partial x^2}+v^2\frac{\partial^2 T}{\partial y^2}+2uv\frac{\partial^2 T}{\partial x\partial y} + \left(u\frac{\partial u}{\partial x}+v\frac{\partial u}{\partial y}\right)\frac{\partial T}{\partial x}+\left(u\frac{\partial v}{\partial x}+v\frac{\partial v}{\partial y}\right)\frac{\partial T}{\partial y}\right), \quad (9)$$

with boundary conditions

$$\begin{aligned} u &= U_w = cx, \quad v = 0, -k\frac{\partial T}{\partial y} = h_f\,(T_w - T)\,,\\ D_A\frac{\partial a}{\partial y} &= k_s a, \quad D_B\frac{\partial b}{\partial y} = -k_s a, \quad \text{at} \quad y = 0,\\ u \to u_e &= ax, \quad a \to a_o, \quad b \to 0, \quad T \to T_\infty \quad \text{as} \quad y \to \infty, \end{aligned} \quad (10)$$

where $a_0 > 0$ is dimensional constant.

Using the following transformations

$$\begin{aligned} u &= cxf'(\eta), \quad v = -\sqrt{c\nu}f(\eta), a = a_0 g(\eta),\\ \theta(\eta) &= \frac{T - T_\infty}{T_w - T_\infty}, \quad \eta = \sqrt{\frac{c}{\nu}}y, b = a_0 h(\eta). \end{aligned} \quad (11)$$

Eq. (3) is satisfied and Eqs. (4), (6), (7), (9) and (10) are given by

$$f''' + Wef''f''' + ff'' - f'^2 - M\,(f' - \lambda) + \lambda^2 = 0, \quad (12)$$

$$g'' + Scfg' - Sck_1gh^2 = 0, \quad (13)$$

$$\delta h'' + Scfh' + Sck_1gh^2 = 0, \quad (14)$$

$$\theta'' + \Pr f\theta' - \Pr\gamma\left(f^2\theta'' + ff'\theta'\right) = 0, \quad (15)$$

and

$$\begin{aligned} f(0) &= 0, \quad f'(0) = 1, \quad g'(0) = k_2 g(0),\\ \theta'(0) &= -\gamma_1(1 - \theta(0)), \quad \text{at} \quad y = 0,\\ f'(\infty) &\to \lambda, \quad g(\infty) \to 1, \quad \theta(\infty) \to 0, \quad \text{as} \quad y \to \infty, \end{aligned} \quad (16)$$

with $Pr, \gamma, \gamma_1, Sc, \delta, \lambda, M$ and k_1, k_2 represent Prandtl number, thermal relaxation time parameter, Biot number, Schmidt number, ratio of diffusion coefficient, velocity ratio parameter, Hartmann number and amount of force of homogenous and heterogeneous reactions respectively. These quantities are represented by

$$\begin{aligned} \Pr &= \frac{\mu C_p}{k}, \quad \gamma = \lambda_1 c, \quad k_1 = \frac{k_c a_0^2}{c}, \ \delta = \frac{D_B}{D_A}, We = U_w\sqrt{\frac{2c}{\nu}}\Gamma,\\ \gamma_1 &= \frac{h_f}{k}\sqrt{\frac{\nu}{a}}, M = \frac{\sigma B_o^2}{c\rho}, \quad Sc = \frac{\nu}{D_A}, k_2 = \frac{k}{D_A a_0}\ \sqrt{\frac{c}{\nu}}, \ \lambda = \frac{a}{c} \end{aligned} \quad (17)$$

with the assumption that diffusion coefficients of chemical classes A and B are of the same magnitude. Eventually, this leads to the fact that D_A and D_B are similar, i.e., $\delta = 1$. So, we have

$$g(\eta) + h(\eta) = 1. \quad (18)$$

From Eqs. (13) and (14), we have

$$g'' + Scfg' - Sck_1g(1 - g)^2 = 0, \quad (19)$$

with

$$g'(0) = k_2 g(0), \quad g(\infty) = 1. \quad (20)$$

Skin friction coefficient and local Nusselt number are defined by

$$C_{fx} = \frac{\tau_w}{\rho u_w^2(x)}, \quad Nu_x = \frac{xq_w}{k(T_w - T_\infty)}, \quad (21)$$

with

$$\tau_w = \mu\left[\frac{\partial u}{\partial y} + \frac{\Gamma}{2}\left(\frac{\partial u}{\partial y}\right)^2\right]_{y=0}, q_w = -k\left(\frac{\partial T}{\partial y}\right)_{y=0}. \quad (22)$$

Dimensionless forms of skin friction coefficient and local Nusselt number are

$$2\sqrt{2}C_{fx}Re_x^{1/2} = f''(0) + Wef''^2(0), \quad N_{u_x}Re_x^{-1/2} = -\theta'(0). \quad (23)$$

3. Numerical solutions

The resulting system of nonlinear ODEs along with boundary conditions is solved iteratively by the shooting method for several values of different parameters. Shooting method is renowned because of its simplicity and low computational cost. This method is more faster in comparison to the finite difference or any other numerical computational technique. On the basis of number of computational experiments, we are considering [0, 7] as the domain of the problem instead of $[0, \infty)$ because for $\eta > 7$, there is no significant variation in the results. We denote f by y_1 , θ by y_4 and g by y_6 for converting the boundary value problem to the following initial value problem (IVP).

$y_1' = y_2$	$y_1(0) = 0,$
$y_2' = y_3$	$y_2(0) = 1,$
$y_3' = \frac{1}{1+We\,y_3}\,(y_2^2 - y_1y_3 + M\,(y_2 - \lambda) - \lambda^2)$	$y_3(0) = r,$
$y_4' = y_5$	$y_4(0) = s,$
$y_5' = \frac{1}{1-\Pr\gamma y_2}\,(\Pr\gamma y_1y_2y_5 - \Pr y_1y_5)$	$y_5(0) = \gamma(1 - y_4(0)),$
$y_6' = y_7$	$y_6(0) = t,$
$y_7' = -Scy_1y_7 + Sck_1y_6(1 - y_6)^2$	$y_7(0) = k_2y_6(0),$

where r, s and t are missing initial guesses. To refine these guesses, we use Newton's method.

4. Results and discussion

Here in this section, we have presented effects of arising prominent parameters on respective distributions with physical insight. Figs. 2 and 3 depict the effect of Williamson fluid parameter We on velocity and temperature profiles respectively. In Fig. 2, it is seen that velocity distribution is decreasing function of Williamson parameter. Physically, higher resistance to the flow of fluid is witnessed due to increase in relaxation time. Eventually, decrease in velocity distribution is observed. Fluid temperature is increased because of high resistance and more collisions of molecules in the fluid. This fact is shown in Fig. 3. The influence of Hartmann number M on velocity profile is displayed in Fig. 4. It is perceived that increasing values of M decrease the velocity distribution. Amplified Lorentz force is noted because of increasing Hartmann number that opposes fluid motion and thus reduction in velocity profile is perceived. The impact of thermal relaxation time γ on temperature field is portrayed in Fig. 5. It is witnessed that temperature profile and its allied boundary layer thickness are diminishing functions of thermal

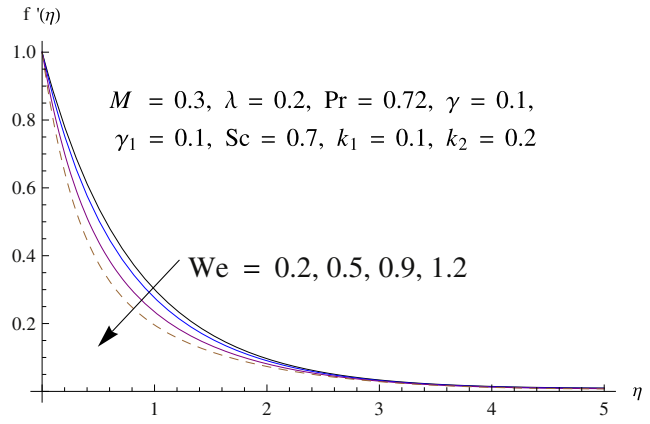

Fig. 2. Influence of *We* on $f'(\eta)$.

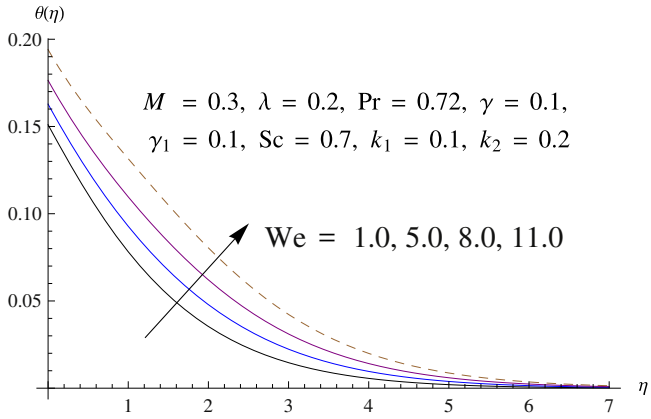

Fig. 3. Influence of *We* on $\theta(\eta)$.

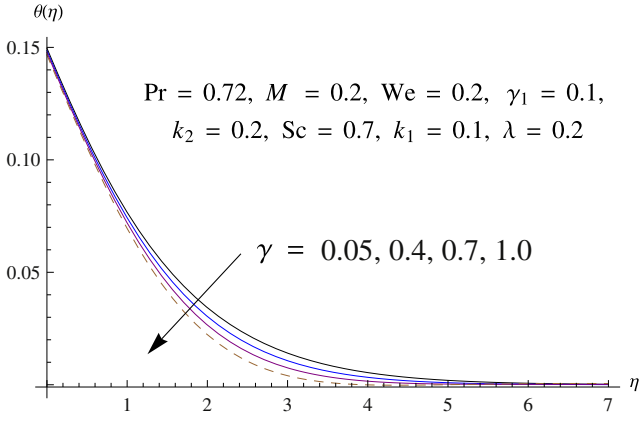

Fig. 5. Influence of γ on $\theta(\eta)$.

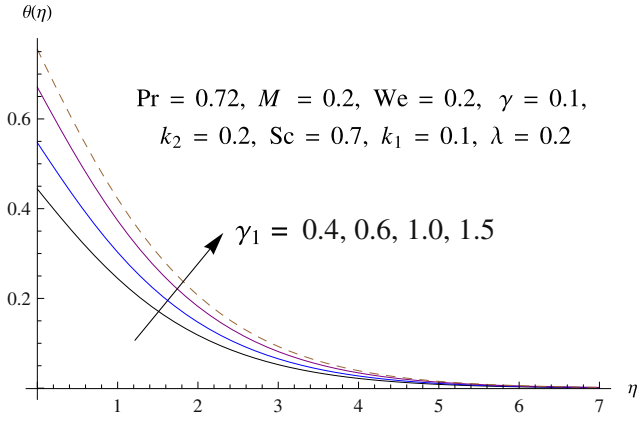

Fig. 6. Influence of γ_1 on $\theta(\eta)$.

relaxation time. Because of growing thermal relaxation time, material particles need additional time to transfer heat to adjacent particles. Physically, non-conducting behavior of material is observed against mounting relaxation time parameter which reduces the temperature field. Fig. 6 epitomize the behavior of Biot number γ_1 on temperature field. Higher values of Biot number upsurge the temperature distribution which correspond to sturdy heat transfer coefficient and eventually augmentation in temperature distribution is observed. Measures of homogeneous and heterogeneous reactions k_1, k_2 on concentration distribution are displayed in Figs. 7 and 8 respectively. In homogeneous reactions, consumption of reactants results in decrease in concentration distribution with escalating values of k_1. But concentration field decreases and increases as it is near and away from the surface for larger values of k_2. Away from the surface, diffusion decreases, and escalation in concentration distribution is witnessed. Increasing values of Schmidt number enhances the concentration field as displayed in Fig. 9. Since, Schmidt number is a quotient of momentum diffusivity to mass diffusivity and because of

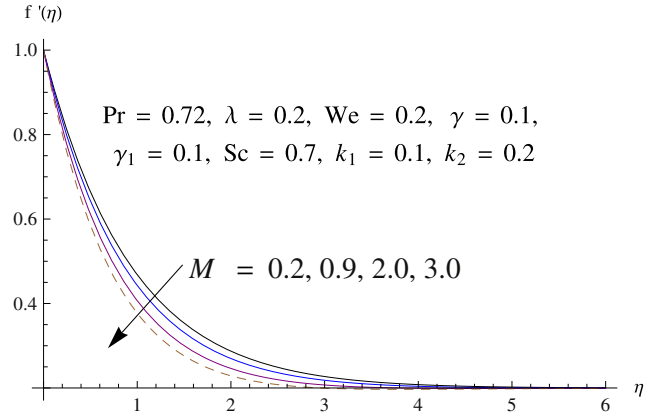

Fig. 4. Influence of *M* on $f'(\eta)$.

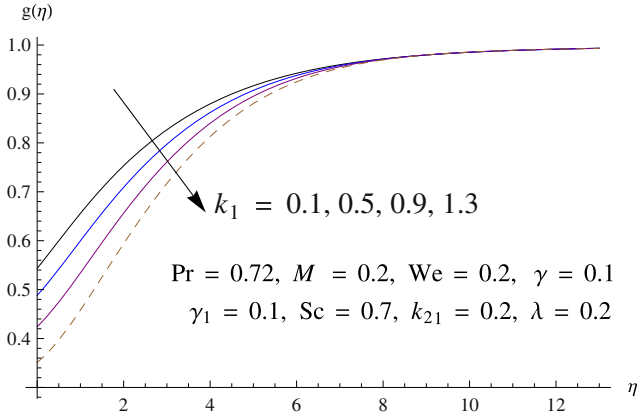

Fig. 7. Influence of k_1 on $g(\eta)$.

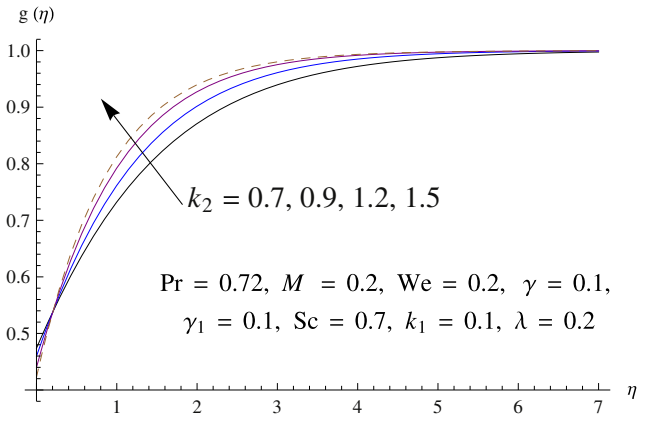

Fig. 8. Influence of k_1 on $g(\eta)$.

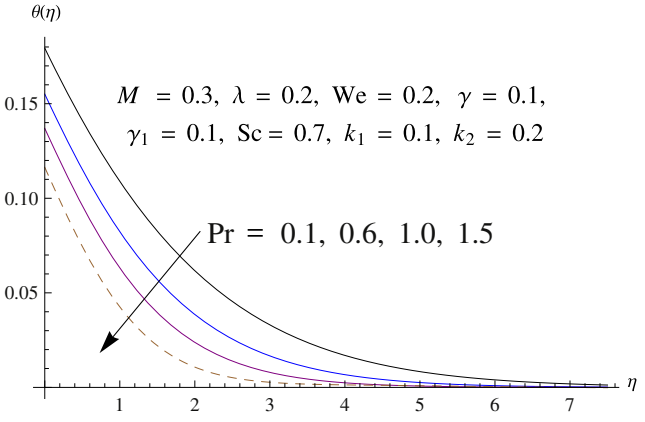

Fig. 11. Influence of Pr on $\theta(\eta)$.

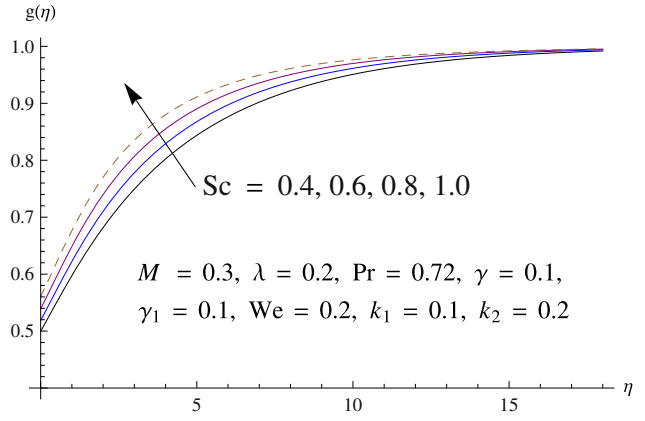

Fig. 9. Influence of Sc on $g(\eta)$.

smaller mass diffusivity mounting concentration field is witnessed. Fig. 10 depicts that higher values of velocity ratio parameter λ, enhances the velocity profile. This is the case when the stretching sheet's velocity is higher than the free stream velocity for both $\lambda > 1$ and $\lambda < 1$. However, for $\lambda = 1$, no boundary layer will be shaped. Impact of Prandtl number Pr on temperature profile is portrayed in Fig. 11. It is perceived that feeble thermal diffusivity is seen for larger Prandtl number which is the basic cause for thinner thermal boundary layer thickness. Fig. 12 is plotted to see the effects of Hartmann number M and thermal velocity ratio parameter λ on skin friction coefficient. It is found that skin friction coefficient is increasing function of both M and λ. Since, the magnetic field is normal to surface there for strength produce by MHD will resist the fluid molecules and enhance the skin friction at the surface. So, defined physical interpretation pretends that skin friction is getting increase due to rise of Hartmann number. Similarly, stagnation ratio parameter also depicts the same behavior that we have achieved for Hartmann number. Since λ is the ratio of free stream velocity to stretching velocity, therefore $\lambda > 1$ illustrates the higher free stream velocity as compared to the stretching velocity and similarly $\lambda < 1$ presents that stretching velocity is greater than the free stream velocity. In Fig. 12, it can be observed that$\lambda = 0$ has low skin friction as compared to the nonzero values of λ. While, skin friction is attaining increasing behavior when stretching velocity is greater than the free stream velocity ($0 < \lambda < 1$). The impact of Prandtl number Pr and thermal relaxation time parameter γ on local Nusselt number is depicted in Fig. 13. It is observed that escalating values of Pr and γ results in mounting local Nusselt number. According to the definition of Prandtl number, it is the ratio of viscosity to the thermal diffusion and so by enhancing the values of Prandtl number, fluid molecules diffuse and rise the thermal conductivity of working fluid. Results plotted in figure describe the similar effects on local Nusselt number according to the definition of Prandtl number. Same increasing effect can be found for Nusselt number with the variation of γ.

Table 1 is constructed to compare various values of Williamson parameter We in limiting case with already published results [38], and all results are found to be in excellent agreement.

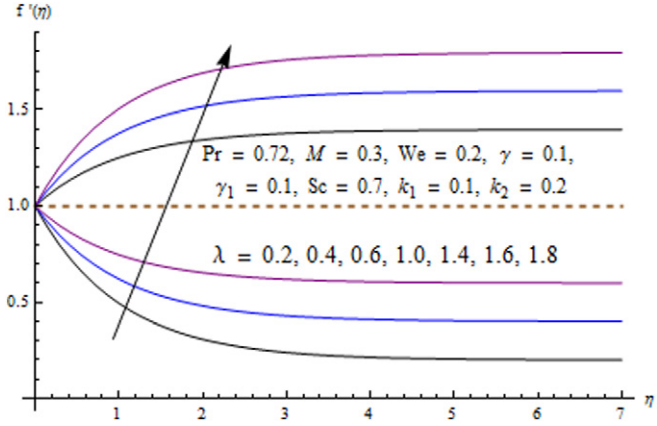

Fig. 10. Influence of λ on $f'(\eta)$.

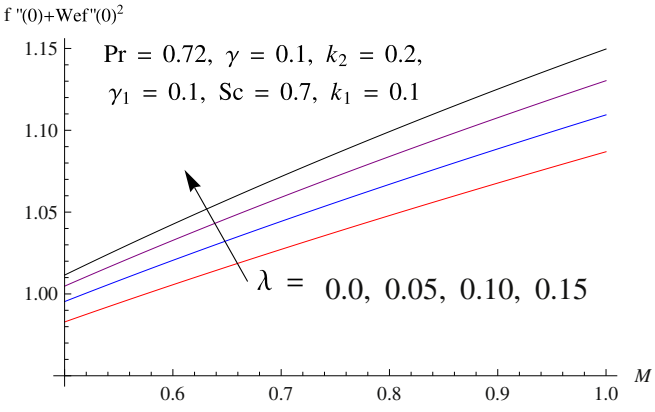

Fig. 12. Influence of M and λ on skin friction.

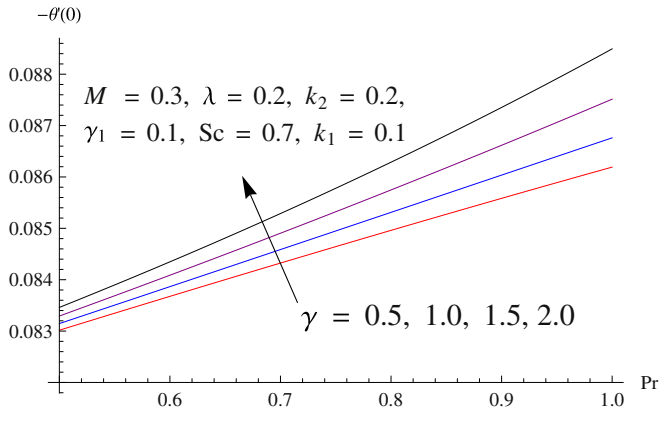

Fig. 13. Influence of Pr and γ on Nusselt number.

Table 1
Comparison of $C_{fx}Re_x^{1/2}$ for various values of *We*.

We	$C_{fx}Re_x^{1/2}$ [38]	Present
0	1	1
0.1	0.976588	0.976586
0.2	0.939817	0.939814
0.3	0.88272	0.88270

5. Final remarks

This effort examined the flow of Williamson fluid under the influence of homogeneous–heterogeneous reactions and Cattaneo–Christov heat flux past a linearly stretched surface. Effects of magnetohydrodynamics with convective boundary condition near a stagnation point are also considered. Shooting method is engaged to find numerical solution of the present study. Salient characteristics of the exploration are as follow:

- Behavior of *We* on velocity and temperature distributions are opposite.
- Influence of *M* and λis similar on skin friction coefficient.
- Numerical results are in an excellent covenant in limiting case to those already explored.
- Effects of k_1 and k_2 on $g(\eta)$ are opposite.
- $\theta(\eta)$ is mounting function of Biot number γ_1.
- *Pr* and γ have diminishing tendency of temperature profile.

Conflict of interest

Authors have no conflict of interest regarding this publication.

Acknowledgments

This research is supported by theKorea Institute of Energy Technology Evaluation and Planning (KETEP) granted financial resource from the Ministry of Trade, Industry & Energy of Korea (No. 20132010101780).

References

[1] M. Turkyilmazoglu, Equivalences and correspondences between the deforming body induced flow and heat in two-three dimensions, Phys. Fluids 28 (2016) 043102.
[2] M. Ramzan, M. Farooq, T. Hayat, J.D. Chung, Radiative and Joule heating effects in the MHD flow of a micropolar fluid with partial slip and convective boundary condition, J. Mol. Liq. 221 (2016) 394–400.
[3] M. Turkyilmazoglu, Three dimensional MHD flow and heat transfer over a stretching/shrinking surface in a viscoelastic fluid with various physical effects, Int. J. Heat Mass Transf. 78 (2014) 150–155.
[4] R. Mehmood, S. Nadeem, S. Masood, Effects of transverse magnetic field on a rotating micropolar fluid between parallel plates with heat transfer, J. Magn. Magn. Mater. 401 (2016) 1006–1014.
[5] S.S. Nadeem, Saleem, Analytical study of third grade fluid over a rotating vertical cone in the presence of nanoparticles, Int. J. Heat Mass Trasnf. 85 (2015) 1041–1048.
[6] M. Turkyilmazoglu, An analytical treatment for the exact solutions of MHD flow and heat over two–three dimensional deforming bodies, Int. J. Heat Mass Transf. 90 (2015) 781–789.
[7] M. Turkyilmazoglu, MHD Fluid flow and heat transfer due to a shrinking rotating disk, Comput. Fluids 90 (2014) 51–56.
[8] S. Nadeem, R. Mehmood, S.S. Motsa, Numerical investigation on MHD oblique flow of Walter's B type nano fluid over a convective surface, Int. J. Therm. Sci. 92 (2015) 162–172.
[9] S. Nadeem, S. Masood, R. Mehmood, M.A. Sadiq, Optimal and numerical solutions for an MHD micropolar nanofluid between rotating horizontal parallel plates, PLoS ONE 10 (6) (2015) e0124016.
[10] M. Ramzan, M. Bilal, Three-dimensional flow of an elastico-viscous nanofluid with chemical reaction and magnetic field effects, J. Mol. Liq. 215 (2016) 212–220.
[11] R.V. Williamson, The flow of pseudoplastic materials, Ind. Eng. Chem. Res. 21 (11) (1929) 1108.
[12] N.S. Akbar, S. Nadeem, C. Lee, Z.H. Khan, R.U. Haq, Numerical study of Williamson nano fluid flow in an asymmetric channel, Results Phys. 3 (2013) 161–166.
[13] S. Nadeem, S.T. Hussain, C. Lee, Flow of a Williamson fluid over a stretching sheet, Braz. J. Chem. Eng. 30 (3) (2013) 619–625.
[14] M.Y. Malik, T. Salahuddin, Numerical solution of MHD stagnation point flow of Williamson fluid model over a stretching cylinder, Int. J. Nonlinear Sci. Numer. Simul. 16 (3-4) (2015) 161–164.
[15] M.Y. Malik, M. Bibi, F. Khan, T. Salahuddin, Numerical solution of Williamson fluid flow past a stretching cylinder and heat transfer with variable thermal conductivity and heat generation/absorption, AIP Adv. 6 (2016) 035101.
[16] T. Hayat, Y. Saeed, S. Asad, A. Alsaedi, Soret and Dufour effects in the flow of Williamson fluid over an unsteady stretching surface with thermal radiation, Z. Naturforsch. A 70 (4) (2015) 235–243.
[17] T. Hayat, A. Shafiq, M.A. Farooq, H.H. Alsulami, S.A. Shehzad, Newtonian and Joule heating effects in two-dimensional flow of Williamson fluid, J. Appl. Fluid Mech. 9 (4) (2016) 1969–1975.
[18] S. Nadeem, S.T. Hussain, Flow and heat transfer analysis of Williamson nanofluid, Appl. Nanosci. 4 (2014) 1005–1012.
[19] T. Salahuddin, M.Y. Malik, A. Hussain, M. Awais, MHD Flow of Cattaneo–Christov heat flux model for Williamson fluid over a stretching sheet with variable thickness: using numerical approach, J. Magn. Magn. Mater. 401 (2015) 991–997.
[20] B.C. Prasannakumara, B.J. Gireesha, R.S.R. Gorla, M.R. Krishnamurthy, Effects of chemical reaction and nonlinear thermal radiation on Williamson nanofluid slip flow over a stretching sheet embedded in a porous medium, J. Aerosp. Eng. 29 (5) (2016) 04016019.
[21] M.A. Chaudhary, J.H. Merkin, A simple isothermal model for homogeneous–heterogeneous reactions in boundary-layer flow. I. Equal diffusivities, Fluid Dyn. Res. 16 (6) (1995) 311–333.
[22] M.A. Chaudhary, J.H. Merkin, A simple isothermal model for homogeneous–heterogeneous reactions in boundary-layer flow. II. Different diffusivities for reactant and autocatalyst, Fluid Dyn. Res. 16 (6) (1995) 335–359.
[23] J.H. Merkin, A model for isothermal homogeneous–heterogeneous reactions in boundary-layer flow, Math. Comput. Model. 24 (8) (1996) 125–136.
[24] W.A. Khan, I. Pop, Effects of homogeneous–heterogeneous reactions on the viscoelastic fluid toward a stretching sheet, J. Heat Transf. 134 (6) (2012) 064506.
[25] S. Shaw, P.K. Kameswaran, P. Sibanda, Homogeneous–heterogeneous reactions in micropolar fluid flow from a permeable stretching or shrinking sheet in a porous medium, Bound. Value Probl. 77 (2013) 2270–2779.
[26] P.K. Kameswaran, S. Shaw, P. Sibanda, P.V.S.N. Murthy, Homogeneous–heterogeneous reactions in a nanofluid flow due to a porous stretching sheet, Int. J. Heat Mass Transf. 57 (2) (2013) 465–472.
[27] S. Mansur, A. Ishak, I. Pop, MHD Homogeneous–heterogeneous reactions in a nanofluid due to a permeable shrinking surface, J. Appl. Fluid Mech. 9 (3) (2016) 1073–1079.
[28] T. Hayat, Z. Hussain, M. Farooq, A. Alsaedi, Effects of homogeneous and heterogeneous reactions and melting heat in the viscoelastic fluid flow, J. Mol. Liq. 215 (2016) 749–755.
[29] T. Hayat, Z. Hussain, A. Alsaedi, M. Farooq, Magnetohydrodynamic flow by a stretching cylinder with newtonian heating and homogeneous–heterogeneous reactions, PLoS ONE 11 (6) (2016) e0156955.
[30] T. Hayat, Z. Hussain, T. Muhammad, A. Alsaedi, Effects of homogeneous and heterogeneous reactions in flow of nanofluids over a nonlinear stretching surface with variable surface thickness, J. Mol. Liq. 221 (2016) 1121–1127.
[31] J. Fourier, Th′eorie Analytique Ee La Chaleur, Paris, 1822.

[32] Cattaneo, Sulla conduzione del calore, Atti Semin. Mat. Fis. Univ. Modena Reggio Emilia 3 (1948) 83–101.
[33] C.I. Christov, On frame indifferent formulation of the Maxwell–Cattaneo model of finite-speed heat conduction, Mech. Res. Commun. 36 (2009) 481–486.
[34] B. Straughan, Thermal convection with the Cattaneo–Christov model, Int. J. Heat Mass Transf. 53 (2010) 95–98.
[35] M. Ciarletta, B. Straughan, Uniqueness and structural stability for the Cattaneo–Christov equations, Mech. Res. Commun. 37 (5) (2010) 445–447.
[36] M. Mustafa, Cattaneo–Christov heat flux model for rotating flow and heat transfer of upper-convected maxwell fluid, AIP Adv. 5 (2015) 047109.
[37] T. Hayat, T. Muhammad, A. Alsaedi, M. Mustafa, A comparative study for flow of viscoelastic fluids with Cattaneo–Christov heat flux, PLoS ONE 11 (5) (2016) e0155185.
[38] S. Nadeem, S.T. Hussain, C. Lee, Flow of a Williamson fluid over a stretching sheet, Braz. J. Chem. Eng. 30 (3) (2013) 619–625.